

## N O T I C E

THIS DOCUMENT HAS BEEN REPRODUCED FROM  
MICROFICHE. ALTHOUGH IT IS RECOGNIZED THAT  
CERTAIN PORTIONS ARE ILLEGIBLE, IT IS BEING RELEASED  
IN THE INTEREST OF MAKING AVAILABLE AS MUCH  
INFORMATION AS POSSIBLE

LANGMUIR PROBE MEASUREMENTS OF DOUBLE-LAYERS  
IN A PULSED DISCHARGE

by

J. S. Levine and F. W. Crawford

NASA Grant NGL 05-020-176

and

NSF Grant ATM 78-08440

(NASA-CR-162845) LANGMUIR PROBE  
MEASUREMENTS OF DOUBLE-LAYERS IN A PULSED  
DISCHARGE (Stanford Univ.) 48 p  
HC A03/MF A01

N80-19954

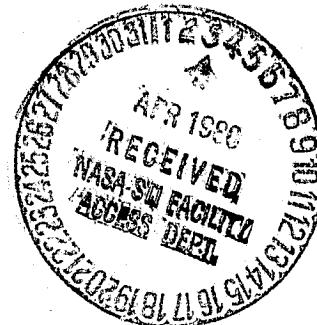
CSCL 201

Unclas  
63/75 47541

SU-IPR Report No. 807

March 1980

Institute for Plasma Research  
Stanford University  
Stanford, California 94305



## CONTENTS

	<u>Page</u>
ABSTRACT . . . . .	1
1. INTRODUCTION . . . . .	2
2. PREVIOUS EXPERIMENTS . . . . .	4
2.1 Low-Pressure Discharges without Magnetic Fields . .	4
2.2 Low Pressure Discharges with Magnetic Fields . . .	7
2.3 Multiple Plasma Devices . . . . .	9
2.4 Summary . . . . .	11
3. DOUBLE-LAYERS IN A STEADY-STATE DISCHARGE . . . . .	13
3.1 Apparatus . . . . .	13
3.2 Observations . . . . .	14
4. DOUBLE-LAYERS IN A PULSED DISCHARGE . . . . .	16
4.1 Pulsing Circuit . . . . .	16
4.2 Time-resolved Diagnostics . . . . .	16
4.3 Observations and Measurements . . . . .	19
5. DISCUSSION . . . . .	22
ACKNOWLEDGMENTS . . . . .	25
REFERENCES . . . . .	26

## FIGURES

<u>Figure</u>	<u>Page</u>
1. Sheaths and double-layers commonly observed in low-pressure discharges . . . . .	28
2. Apparatus used in previous double-layer investigations:	
(a) Mercury-vapor positive column discharge with tapered sections, . . . . .	29
(b) Linear discharge in a magnetic field, . . . . .	29
(c) Diffusion column in a magnetic field, . . . . .	30
(d) Double-plasma device, . . . . .	30
(e) Triple-plasma device. . . . .	30
3. Apparatus for double-layer investigation . . . . .	31
4. Current-voltage characteristics of an argon positive column. (Double-layer formation is associated with the abrupt transition in the 0.8 mTorr curve.) . . . . .	32
5. Steady-state double-layer.	
(a) RF emission on cathode and anode sides of a double-layer ( $P_{\text{CATH}} = 2.6$ mTorr; $P_{\text{ANODE}} = 0.74$ mTorr; $U = 168$ V; $I = 7.9$ A), . . . . .	33
(b) Axial variation of the floating potential of a Langmuir probe in the vicinity of a double-layer ( $P_{\text{CATH}} = 2.2$ mTorr; $P_{\text{ANODE}} = 0.51$ mTorr; $U = 145$ V; $I = 5.0$ A) . . . . .	33
6. (a) Circuit for the pulsed discharge, . . . . .	34
(b) Detail of the transistor switch (Resistances are in $\Omega$ ). . . . .	35
7. (a) Circuit for probe diagnostics in the pulsed discharge. ( $X$ , $Y_1$ and $Y_2$ are the axes of XY recorders. Resistances are in $\Omega$ ). . . . .	36
(b) Sequencing diagram of timing pulses (Reference point is trigger output of Pulse Generator 1) . . . . .	37
8. Microwave interferometer . . . . .	38

FigurePage

9. Pulsed double-layer: RF emission on cathode and anode side of the double-layer, and the discharge current  
( $P_{\text{CATH}} = 1.1 \text{ mTorr}$ ;  $P_{\text{ANODE}} = 0.57 \text{ mTorr}$ ). . . . . 39
10. RF growth and saturation with double-layer formation  
(1.8 MHz ; 300 kHz IF bandwidth;  
 $P_{\text{CATH}} = 1.8 \text{ mTorr}$ ;  $P_{\text{ANODE}} = 0.18 \text{ mTorr}$ ). . . . . 40
11. Low frequency RF generation near double-layer  
( $P_{\text{CATH}} = 1.8 \text{ mTorr}$ ;  $P_{\text{ANODE}} = 0.18 \text{ mTorr}$ ). . . . . 41
12. Time-resolved measurements of space potential, electron temperature and density on the cathode (open symbols) and anode (closed symbols) sides of a double-layer  
( $P_{\text{CATH}} = 0.96 \text{ mTorr}$ ;  $P_{\text{ANODE}} = 0.44 \text{ mTorr}$ ). . . . . 42
13. Pulsed double-layer: Electron density, discharge current and RF emission on cathode and anode sides  
( $P_{\text{CATH}} = 0.96 \text{ mTorr}$ ;  $P_{\text{ANODE}} = 0.44 \text{ mTorr}$ ). . . . . 43
14. Discharge current for a strong, unstable double-layer  
 $P_{\text{CATH}} = 1.1 \text{ mTorr}$   $P_{\text{ANODE}} = 0.32 \text{ mTorr}$  . . . . . 44

LANGMUIR PROBE MEASUREMENTS OF DOUBLE-LAYERS  
IN A PULSED DISCHARGE

by

J. S. Levine and F. W. Crawford

Institute for Plasma Research  
Stanford University  
Stanford, California 94305

ABSTRACT

Langmuir probe measurements have been carried out which confirm the occurrence of double-layers in an argon positive column. Pulsing the discharge current permitted probe measurements to be performed in the presence of the double-layer. Supplementary evidence, obtained from DC and pulsed discharges, indicated that the double-layers formed in the two modes of operation were similar. The double-layers observed were weak and stable; their relation to other classes of double-layers are discussed, and directions for future work are suggested.

## 1. INTRODUCTION

A double-layer consists of two space-charge layers in close proximity, one positively charged and one negatively. Although several kinds of double-layers have been studied experimentally and theoretically since Langmuir (1929), there has been a recent concentration of interest on the "free" double-layers with which this paper is concerned (see Torven 1979; Carlqvist 1979; Levine & Crawford 1980, and references therein). To aid in distinguishing them from more familiar space-charge layers (sheaths), figure 1 shows a variety of such phenomena observed in laboratory plasmas.

First, there is a category of space-charge layers that form in the vicinity of boundaries (Self 1965) and electrodes (Langmuir 1929; Crawford & Cannara 1965; Prewett and Allen 1976). Strong electric fields obtain within such sheaths, while the bulk of the plasma is relatively field-free. There may be either a single space-charge layer, with an approximately equal and opposite charge on the bounding surface, or two approximately equal and opposite space-charge layers constituting a double-layer next to the boundary.

Second, there are double-layers that form within the plasma volume, for example, in a plasma which has an abrupt change of section (Crawford & Freeston 1963; Andersson *et al.* 1969; Sandahl 1971; Jacobsen & Eubank 1973). This type of sheath, which may be observed as the result of a wall constriction, consists of two space-charge layers, and is the transition between two plasmas with distinctly different characteristics (electron temperature, number density, etc.), the characteristics being determined by the column radii. Double-layers may also occur in columns of uniform cross-section at the heads of moving or standing striations (Rayment & Twiddy 1969). They are then generally periodic in space and time, and occur for discharge parameters that can be predicted approximately by linear ionization instability theory (Oleson & Cooper 1968).

The double-layers which we shall term "free" occur within the plasma volume, and have been observed in low-pressure discharges of uniform cross-section at high current densities. There is a single potential discontinuity, rather than a periodic structure, and RF emissions are associated with the double-layer. So far, neither the origins of these instabilities, nor their relation to the double-layer itself, have been clearly demonstrated or predicted.

Studies of free double-layers have been conducted with low pressure discharges, both with and without axial magnetic fields, and with multiple plasma devices in which long enough Debye lengths are obtainable for the spatial structure of the double-layer to be resolved. In § 2, we shall review the literature describing these experiments. As yet, no direct measurements of the potential difference across a double-layer in a positive column have been reported. To fill this gap, Langmuir probe measurements of a double-layer have been made in a low-pressure argon positive column and will be described in §3 and §4. The results, and possible mechanisms for free double-layers, are discussed in §5 .



## 2. PREVIOUS EXPERIMENTS

### 2.1. Low-Pressure Discharges without Magnetic Fields

Torvén & Babić (1971) have described the onset of a free double-layer in a mercury-vapor positive column discharge [see figure 2(a)]. They observed that a rapid current drop occurred when the current approached a pressure-dependent limit, at which the average ionization degree was about 5%. A 200 mH inductor was required in the external circuit to maintain the discharge, and caused overvoltage pulses of 1200 V at the anode, of approximately 10  $\mu$ s duration, 100  $\mu$ s apart. A dark space separating the column into two sections of different luminosity (blue on the cathode side and red on the anode side) could be observed for suitable choices of experimental parameters. Investigations with RF and temperature probes outside the column suggested that most of the voltage drop during the overvoltage surges was localized in the vicinity of the dark space (Babić, Sandahl & Torvén 1971), implying the existence of a double-layer.

The position of the double-layer could be controlled by local heating of a tube containing a quiescent column before raising the current until overvoltages occurred. Langmuir probe measurements in the heated region showed that a local maximum in the plasma potential developed there before the double-layer appeared.

No Langmuir probe measurements made in the presence of a double-layer were presented; the localization of the double-layer was inferred from measurements external to the column, and the potential drop across the double-layer was inferred from the increase in the anode-to-cathode potential difference. The experiments did not establish whether the double-layers were inherently unstable, or the external circuit caused the observed relaxation oscillations.

In a more detailed investigation, Babić & Torvén (1974) studied the effect of circuit inductance,  $L$ , on the magnitude and duration of the overvoltage surges. They reported that a decrease in  $L$  produced an increase in the current drop,  $\Delta i$ , associated with the surges, and a slight increase in the surge duration,  $\Delta t$ , so that the overvoltage,  $V \approx L\Delta i/\Delta t$ , was approximately independent of  $L$ . However, if the inductance was too low, the discharge was extinguished.

The high current density required for double-layer formation necessitated large cathode and anode vessels connected by a narrow (1 cm radius)

section [see figure 2(a)]. A visible constriction sheath formed when the transition was abrupt, while gradually tapered sections produced no visible sheath. Babić & Torveń (1974) found that double-layers could be formed regardless of the type of transition, although the abrupt transition produced more low-level fluctuations in the anode voltage and in the RF emissions from the plasma.

Three types of wave phenomena were observed, using capacitive probes, at current levels below double-layer onset. Two appeared to unrelated to double-layer formation, but connected rather with the cathode and anode tapers, and could be suppressed by application of a weak magnetic field (some tens of Gauss) over a short length of the discharge. The third type of wave seemed to be related: at discharge parameters of about 8.8 A and 80 V, within a 20 cm region near the middle of the narrow section, voltage pulses grew convectively out of the background fluctuations on the cathode side to a level of about 10 V, and then decayed into low level fluctuations of about 1 V. The pulses propagated within this region towards the anode, with a velocity close to the ion sound speed ( $\sim 10^3$  m/s); no time delay was observable between the signal measured on the anode side of this region and the anode voltage variations, which showed the same time dependence, some 120 cm away. The pulses repeated every few hundred  $\mu$ s, originating at different points within the 20 cm region. At slightly higher current and voltage, about 10 A and 85 V, but still without the visually evident double-layer formation, the spatial structure of the RF emission changed. Background noise changed abruptly (in about 1 cm) to large voltage pulses that appeared simultaneously on the anode and at all points between. This discontinuity occurred at random locations in a 10 cm length within the 20 cm region referred to above. Babić & Torvén (1974) interpreted these observations as evidence for double-layers that formed, on an overvoltage pulse-by-pulse basis, at differing locations within the distributed region.

Increasing the current and voltage produced a rapid load-line shift to higher voltage and lower current, about 9.5 A and 100 V. The double-layer became visually evident, with the RF jumping from about 1 V to 100 V, from about 0.5 cm on the cathode side to 0.5 cm on the anode side of the double-layer. This was taken to be a double-layer that formed consistently at the same location. Increasing the current further resulted in larger

voltage pulses, but intense wall heating, a few cm on the anode side of the double-layer, and the risk of melting the tube limited the current to about 15 A.

Babić & Torvén (1974) found that with equal neutral pressures (measured with ionization gauges) in the anode and cathode gas reservoirs, the wall mass flux [measured with wall probes (Torvén & Babić 1973)] at the anode end of the narrow section was always less than at the cathode end. With pressures adjusted to equalize the mass fluxes at the ends of the narrow section, the mass flux to the wall in the middle was a few per cent lower than at the ends. The balancing procedure was used only up to currents at which double-layers first appeared, maintaining an equivalent pressure of 0.66 mTorr. After that, the gas reservoir pressures were kept constant. Balancing the wall mass flux was found to be important: no visible double-layer formed in the unbalanced column, although other suggestions of double-layer occurrence were observed, i.e. high voltage surges and discontinuities in the RF fluctuations measured with the capacitive probes. The RF discontinuities occurred in the cathode (anode) taper when there was an increasing (decreasing) wall mass flux, from the cathode to the anode. The foregoing observations were interpreted by Babić & Torvén (1974) as distributed double-layers, as before.

Once formed in the balanced column, the visible double-layer could be moved short distances by varying the axial inhomogeneities. When moved across a wall flux probe, a major drop in the reading [50% is the uncorrected data (Torvén & Babić 1973)] was observed from the cathode to the anode side of the double-layer. This is reminiscent of the neutral density drop measured across a constriction sheath by Sandahl (1971).

Although no Langmuir probe measurements were made in the presence of the visible double-layer, some were made for currents and voltages where pulses propagating at the ion sound speed were observed, and below. Temperatures of 10-14 eV were reported, which are considerably in excess of the 5-6 eV predicted by Ilić (1973) for a homogeneous mercury-vapor positive column at the pressure-radius product pertinent to this experiment (0.66 mTorr cm). Values of the drift-to-thermal velocity ratio approaching unity were estimated for positions on the anode side of the pulse growth region. This figure was based on a temperature of 11 eV, which fitted the probe characteristic only near space potential. Using the average temperature of 14 eV, the ratio is reduced to 0.9. On the cathode side

of the pulse growth region, the drift-to-thermal velocity ratio was 0.65. The difference in space potential of the two probes, centered 42 cm apart within the narrow section, increased from 16 V at 6 A and 75 V to 22 V at 8.8 A and 80 V. By monitoring one probe while moving the other radially, it was demonstrated that the probes distorted the plasma at these discharge parameters. Further, the double-layer tended to form at the probes.

Experiments by Babić & Torvén (1974), in tubes of various diameters (1, 2 and 3 cm), indicated that a critical parameter for double-layer formation is the current density. This was studied further by operating the column at a current density lower than that for double-layer onset and using an axial magnetic field (50-200 Gauss) to contract the discharge locally. A visible double-layer and a spatial discontinuity in the RF emission occurred within the contracted region.

Armstrong & Torvén (1974) and Armstrong (1975) investigated hydrogen and deuterium positive columns at low pressure (about 10 mTorr) and high current density (about  $1 \text{ A/cm}^2$ ). They observed high voltage pulses at the anode, lasting a few  $\mu\text{s}$ . Using two capacitive probes, a 10 cm length of the column was found that showed only low level fluctuations on the cathode side and high voltage pulses on the anode side, identical to those observed at the anode. The point closest the cathode at which a given pulse was observed varied, but in all cases the pulse was observed simultaneously at all points closer to the anode. The measurements in hydrogen and deuterium parallel those in mercury-vapor with one notable exception: pulse propagation at the ion-acoustic velocity at discharge parameters immediately below those for double-layer formation could be observed only in isolated cases.

## 2.2. Low Pressure Discharges with Magnetic Fields

The study of double-layers in discharges without magnetic fields is complicated by the surrounding walls which tend to outgas, and even to melt, in the presence of a double-layer. These difficulties can be greatly reduced by use of an axial magnetic field.

Lutsenko, Sereda & Kontsevoi (1976) have made observations suggestive of double-layers in high power pulsed discharges (10-25 kV delivered by an  $0.4 \mu\text{F}$  capacitor). They studied pre-ionized plasma columns ( $n \sim 1-5 \times 10^{12}/\text{cm}^3$ ) in hydrogen, argon and air ( $p \sim 2-5 \times 10^{-2}$  mTorr) in a magnetic

field of 0.2 to 0.5 T [see figure 2(b)]. Instead of the 2-3  $\mu$ s usually found necessary to discharge the capacitor, conditions could be found that required 10-20  $\mu$ s to discharge it. After an initial current burst of about 1000 A, lasting 1-2  $\mu$ s, the current dropped rapidly to nearly zero during a pause of several  $\mu$ s. This behavior repeated for several cycles until the discharge current became oscillatory, and the capacitor was rapidly discharged. Capacitive probes indicated formation of a cathode sheath in the first 2  $\mu$ s across which the entire discharge voltage was dropped. The sheath then detached itself from the cathode, and moved toward the anode at  $10^3$ - $10^5$  m/s, moving fastest immediately after a current decrease, then slowing down until the next current increase. When the free double-layer formed, the density at the cathode had risen to about  $10^{13}/\text{cm}^3$ , decreasing to  $10^{11}/\text{cm}^3$  along the length of the chamber. An electron beam formed, and broadband RF emissions were observed in the range 50 MHz - 10 GHz. On some occasions, the double-layer was observed to move a few cm toward the cathode near the end of a low current period. This backward displacement was smaller in a heavier gas. Increasing the capacitor voltage shortened the periods of low current, until they disappeared above 25 kV. When the initial plasma density exceeded  $5 \times 10^{12}/\text{cm}^3$ , the cathode sheath no longer detached itself from the cathode. Increasing the magnetic field from 0.2 to 0.5 T had no important effect on the formation of the double-layer, though it did improve the reproducibility of the results.

Andersson (1978) and Torvén & Andersson (1979) observed an anode sheath moving from the electrode into the plasma. They studied a magnetically confined (50-1500 Gauss) mercury-vapor column (0.01-0.10 mTorr) with plasma density  $10^8$ - $10^9/\text{cm}^3$ . The plasma was produced in an external discharge (without a magnetic field) and diffused into the magnetized section [see figure 2(c)]. The anode could be left floating, or biased to draw current. For small voltage increases above floating potential, the anode acted as a Langmuir probe, with a clearly marked current saturation at space potential. When the bias voltage was increased substantially above space potential, a visible discontinuity, across which most of the potential difference of the anode and plasma was dropped, moved off the anode surface and into the plasma. The anode current was then no longer saturated. The double-layers could be formed for any choice of series resistance (in the anode bias circuit) between the limits of constant voltage (small resistance) to constant current (high resistance).

The potential on the low potential side of the double-layer was approximately time independent, whereas the potential on the high potential side fluctuated by as much as 30%. The voltage fluctuations appeared simultaneously at all points between the double-layer and the anode. Back and forth motion of the double-layer of a few cm was observed at about 300 m/s. No naturally-occurring pulse propagation at the ion acoustic velocity was observed, though for some parameters, waves deliberately excited in the discharge propagated at about 3000 m/s, a plausible ion-acoustic speed.

Measurements with emissive probes, adjusted so that floating potential was within a few volts of space potential, indicated  $e\phi/T_e \sim 10$ , and a double-layer thickness of about  $30 \lambda_D$ , where the electron temperature on the low potential side of the double-layer,  $T_e \sim 2$  eV, has been used to calculate the electronic Debye length,  $\lambda_D \sim 0.4$  mm. Temperatures measured on the high potential side of the double-layer were 10-20 eV. The plasma between the double-layer and the anode must have been supported by volume ionization, since no ions from the external discharge had sufficient energy to penetrate the double-layer. The conversion of the anode sheath to a double-layer, requiring the creation of a positive space-charge layer, occurred under conditions for which ionization within the anode sheath itself was sufficient to create such a layer (Torvén & Andersson 1979).

### 2.3. Multiple Plasma Devices

Quon & Wong (1976) investigated double-layers in an argon plasma ( $p \sim 0.1$  mTorr) by use of a double-plasma device consisting of two electrically isolated chambers separated by two wire grids [see figure 2(d)]. Plasma, produced in the source chamber by a set of hot filaments, drifted into the target chamber under the influence of electric fields produced by the grids. The Debye length was long enough,  $\lambda_D \sim 1.7$  mm ( $n \sim 10^8/\text{cm}^3$ ,  $T_e \sim 3.7$  eV), for the grids to control the plasma effectively, and for the internal structure of the double-layers to be investigated with probes. A stable double-layer formed,  $20-30 \lambda_D$  wide, when the electron drift energy exceeded the electron thermal energy,  $W_e > T_e$ .

Langmuir probes and ion energy analyzers confirmed the existence of free and trapped electrons and ions (see, e.g. Levine & Crawford 1980). The energy gained by charged particles crossing the double-layer was measured to be within 10% of the measured potential jump. The trapped electron

population was constituted by accelerated electrons thermalized by beam-plasma interactions. Ions accelerated by the double-layer were reflected by the grids, forming the trapped ion population. These were found to be essential for the existence of the double-layer, as was seen by biasing a grid to collect, rather than reflect, them.

Temporal evolution of the double-layer was studied by pulsing the potential difference between the two chambers. The electric field in the middle of the target chamber was monitored with a probing electron beam [see figure 2(d)] and plasma potential in the target chamber was found from time-sampled Langmuir probe data. It was observed that a potential pulse transformed from a propagating soliton-like structure, across which the potential difference was nearly zero, to a double-layer. During the transformation, spatial oscillations were evident on the high potential side. The double-layer formed in 30-60  $\mu$ s. This was 5-10 ion plasma periods (Quon & Wong 1976), but may be significant instead as the time required for accelerated ions to reflect from the grids and form the trapped ion population. Double-layers could be formed with  $W_e \leq 4.5 T_e$ . For larger initial drift energies, the double-layers broke up into intense field spikes with large-amplitude ion density fluctuations. Although not directly reported, the maximum value for  $e\phi/T_e$  appears to have been 4-5.

Coakley et al. (1978) and Coakley & Hershkowitz (1979) have shown that stable double-layers with much larger values of  $e\phi/T_e$  could be produced. They used a triple-plasma device with two source chambers and a central target chamber [see figure 2(e)], allowing them to produce a population of trapped electrons without relying on thermalization of the free electrons on the high potential side of the double-layer. With typical operating parameters (0.03-0.30 mTorr argon pressure;  $3 \times 10^7/\text{cm}^3$  density and 1.0 eV electron temperature), values of  $e\phi/T_e \sim 18$  could easily be produced, with one observation as high as 22. The electron beam formed by acceleration through the double-layer could be followed, by Langmuir probes, for  $100 \lambda_D$  (10 cm) without thermalization. Although no direct measurements of the ions were reported, an indirect measure showed that the ions entered the double-layer on the high potential side with a drift velocity very near to the ion acoustic speed, as would be required by the Bohm (1949) condition. Measurements made off the axis of symmetry

showed the three-dimensional structure of the double-layer; the largest potential difference occurred on-axis, though the highest electric field was slightly off-axis.

The care required in interpreting probe data was strikingly indicated by the observation of pseudo-double-layers (Coakley & Hershkowitz 1979). Here the results of measurements with a single Langmuir probe, moved through the system, indicated the presence of a double-layer. However, when there were two probes it was evident that there were two metastable states for the discharge, between which the plasma switched as the probe was moved. In neither state was there a double-layer.

As in the double-plasma device (Quon & Wong 1976), the trapped ion population determined the characteristics of the double-layer. By varying a grid bias, which served as a potential barrier separating the chambers, the double-layer could be moved within the target chamber and its amplitude varied.

The sensitivity of the double-layer to perturbation was indicated in this experiment. If the high-energy primary electrons in the source chamber on the low potential side of the double-layer, which produced the free electron and trapped ion populations, were not kept out of the target chamber, double-layers with  $e\phi/T_e$  of only 5-8 formed. Since these primary electrons were a low density, high energy population, their effect was thought to be to produce extra plasma at the double-layer (Coakley & Hershkowitz 1979). This conjecture was supported by a modified experiment, with a 50 Gauss magnetic field (Coakley, Johnson & Hershkowitz 1979). As the number of primary electrons allowed to enter the target chamber increased, the double-layer moved toward the free electron source chamber and decreased in amplitude. A numerical calculation that included charge creation within the double-layer gave results in qualitative agreement with their observations.

#### 2.4. Summary

Double-layers have been found to be salient features of a variety of plasma devices: forming in quiescent triple-plasma devices, in the slightly noisier double-plasma devices, and in relatively noisy positive columns and magnetically confined arcs. In the former, the double-layer is distinguished only by the localization of the potential difference applied across the target chamber. In contrast, the external circuit for a positive column determines only the load line (rather than the



potential difference) along which the discharge must operate. The very existence of the large potential difference observed across the discharge is thus a separate effect, reflecting on the current carrying capacity of the discharge. Although the double-layers, considered as potential structures existing self-consistently with charged particle populations (Levine & Crawford 1980), are similar in these various discharges, the physical mechanisms creating the particle populations are likely to be different.

It seems clear that the plasma in which double-layers form is inhomogeneous even before formation. This is evident in the magnetically confined discharges (Lutsenko, Sereda & Kontsevoi 1976; Andersson 1978; Torvén & Andersson 1979) in which double-layers evolved from electrode sheaths, and in the multiple plasma devices (Quon & Wong 1976; Coakley *et al.* 1978; Coakley & Hershkowitz 1979; Coakley, Johnson & Hershkowitz 1979) in which plasmas of differing characteristics were purposely created. It is less clear in the positive column of Babić & Torvén (1974), though they report that the wall mass flux at the middle of the column, where the double-layers formed, was a few per cent lower than at the ends.

Although the potential differences and localization of double-layers have been measured directly in multiple plasma devices, they have only been inferred from external measurements in positive columns. The experiments to be described here have been designed to supply the direct measurements needed to complement the previous positive column measurements. Simultaneous measurements have been made with two Langmuir probes, one on each side of a double-layer, to exclude the possibility mentioned in §2.3 of measuring pseudo-double-layers (Coakley & Hershkowitz 1979).

### 3. DOUBLE-LAYERS IN A STEADY-STATE DISCHARGE

#### 3.1. Apparatus

Free double-layers have been investigated with the apparatus shown in figure 3. To obtain sufficiently high current density for generating double-layers, a reduction of cross section was needed in the positive column region. Both transitions from 5.1 cm diameter to the 86 cm long 2.5 cm diameter section, and the reduced section itself, were made from a single piece of glass, so that O-ring seals are required only between the larger glass pieces. The indirectly-heated oxide cathode is 7.6 cm in diameter. The anode is a 2.5 cm diameter, 1.9 cm long, water-cooled molybdenum cylinder. To ensure electrical isolation, the anode is cooled by an ungrounded, recirculating water system.

The neutral gas pressure can be measured at each end of the column by a Pirani thermal conductivity gauge and an ionization gauge. Base pressure for the tube is  $10^{-6}$  Torr; two to three orders of magnitude below typical operating pressures. Argon is leaked into the system at both ends above the diffusion pump gate valves, which are kept slightly open.

Power for the discharge is supplied by a 10 kW DC power supply which is operable in 10 A/1 kV or 20 A/500 V modes. The discharge is started with the aid of a Tesla coil, with a 500  $\Omega$  series resistor. Once started, the load resistor is switched to 25  $\Omega$ . This is small enough to allow high currents to be drawn at moderate applied voltages but large enough so that the incremental resistance seen by the power supply is always positive. The discharge current is measured from the voltage drop across a 0.1  $\Omega$  series resistor between the cathode and ground.

There are two plane Langmuir probes, facing the cathode, in the system (see figure 3). They were made by first beading the tip of a tungsten wire in a hot flame. An insulating coating was then applied to cover the metal completely, and a flat face was machined off to the desired dimension, 1 mm<sup>2</sup>.

One probe is movable radially at a fixed axial position 15 cm from the 5.1 to 2.5 cm diameter transition at the cathode end of the tube. The insulating material on it is glass. In our experiment, this probe was either positioned on axis, or withdrawn from the system.

The other probe is movable axially by means of a motor drive over a total travel of 84 cm. It has been designed to withstand high temperature. The insulation on the probe tip is alumina. Current is carried through

the 160 cm length of the probe by a tungsten wire inside a ceramic tube, the outside of which is coated with silver paint for a ground shield. The ceramic tube is contained, in turn, by a 3 mm diameter composite tube. This other jacket is mostly glass, with the last 20 cm before the probe tip being quartz and ending with a direct quartz-to-metal vacuum seal. The vacuum feed-through at the anode flange is a Wilson seal, consisting of two gaskets with a pumping port between them, which is connected to a roughing pump. The probe can be moved without noticeable increase in the neutral pressure, even when the tube is at  $10^{-6}$  Torr.

### 3.2. Observations

The current-voltage characteristic of the discharge changed significantly as the neutral pressure was varied around 1 mTorr, for typical parameters of 1-10 A and 100-300 V. As shown in figure 4, the characteristic changed from a flat curve, with the anode-to-cathode voltage drop nearly independent of current, to a smoothly rising voltage as the pressure decreased from 1.2 to 0.7 mTorr. In a narrow range of intermediate pressures, the voltage rose slowly at low currents until a critical current was reached. At this point, the discharge became current limited, with the operating point jumping along the circuit load-line to higher voltages and lower currents.

The intermediate pressure range is that for double-layer formation. Numerous other changes within the column accompany the onset of current limitation. At some location within the narrow section of the tube, the discharge color changes from red, on the cathode side, to bright blue on the anode side. The transition is very abrupt, with no visually evident width. Intense wall heating occurs at this point and, if the double-layer is allowed to remain for more than a few seconds, the wall begins to glow. On a few occasions, the glass cracked or melted under the thermal stress. Such effects can be avoided by water-cooling the tube, or by pulsing the discharge. For reasons which will become clear below, we have preferred the latter solution.

The position at which the double-layer formed was found to be repeatable at any given neutral gas pressure. Increasing the power supply voltage increased the discharge voltage, since the double-layer limited the discharge current (see figure 4), and moved the double-layer a short distance toward the cathode (a few centimeters at most). Although the

pressure range within which the double-layer formed was narrow, so that only small variations in pressure could be made, within this range varying the pressure at either end of the column had the effect of moving the double-layer a few centimeters, always towards the lower pressure end. While the double-layer could be formed with equal neutral pressures at the ends of the column, it formed more readily with a higher pressure at the cathode end (1-2 mTorr) than at the anode end (0.2-0.4 mTorr), and was never observed in the opposite situation.

RF emission was measured by winding a single loop of wire round the outside of the column, and monitoring the signal on an oscilloscope. Such probes couple capacitively to the surface charge density on the inside of the glass (Babić & Torvén 1974), and are thus sensitive to fluctuations in the radial current in the discharge, but not in the axial current. The RF emission was observed to be much more intense on the anode side of the double-layer than on the cathode side [see figure 5(a)]. The RF level was constant from the cathode end of the narrow section up to the double-layer and constant again at a higher level from the double-layer to the anode end of the narrow section.

The change in potential across the double-layer was measured by monitoring the floating potential of the axially movable probe as it was pulled from the cathode side of the double-layer to the anode side. The result, shown in figure 5(b), must be interpreted with care. First, the double-layer was actually much narrower than shown; as the probe was pulled through the double-layer, they moved together for about a centimeter, the double-layer then returning to its undisturbed position. Second, the positive slope in the floating potential, on the anode side of the double-layer, may be partly due to secondary electron emission from the probe. Such emission could result from bombardment by electrons that have just been accelerated by about 10 V through the double-layer. This bombardment was strong enough to cause the alumina insulation on the shank of the probe to glow bright red after only a few seconds. The heating of the probe indicated when the probe was on the anode side of the double-layer, but unfortunately the probe was damaged beyond further use so quickly that detailed measurements of the space potential, temperature and density, of the plasma could not be made. This experience constituted the principal reason for pursuing the experiments in a pulsed discharge.

#### 4. DOUBLE-LAYERS IN A PULSED DISCHARGE

##### 4.1. Pulsing Circuit

The circuit shown in figure 6(a) was used to apply current pulses to the discharge. The input switching signal is electrically isolated from the rest of the circuit by an opto-electronic isolator whose amplified output controls the base current for a pair of power transistors [see figure 6(b)]. The base current is supplied by batteries, so that the switching circuit has no external voltage reference and can be placed at any point in the discharge circuit. Tests with resistive loads showed that 20 A could be switched on in about 2  $\mu$ s and off in less than 1  $\mu$ s.

To pulse the discharge current from a low level to a high level, the transistor switch was connected in series with a 1.5-11  $\Omega$  variable resistor, and placed in parallel with the 25  $\Omega$  ballast resistor used for the DC measurements. Thus, the current was pulsed by decreasing the resistance in series with the discharge.

##### 4.2. Time-resolved Diagnostics

If no integration is required for noise suppression, phenomena can be examined pulse by pulse on an oscilloscope. If integrated data are required, a boxcar integrator can be used. This averages a repetitive input signal resolved to a small time aperture occurring at an adjustable delay time after a reference pulse synchronized with the input signal. This method is useful when the response time of the measuring instrument is shorter than the time scale of the phenomenon being investigated. When the response time of the measuring instrument is too long for use of a boxcar integrator, time resolution can be accomplished by gating the input signal appropriately before introducing it into the measuring instrument. Noise suppression is then obtained by virtue of the integration time of the measuring instrument. These general methods have been used in the various diagnostic techniques discussed below.

###### (i) Current Monitor

The time dependence of the discharge current, determined by the voltage drop across a 0.1  $\Omega$  series resistor [see figure 6(a)] could be monitored on an oscilloscope, or many current pulses could be averaged and recorded with a boxcar integrator.

(ii) Langmuir Probes

Probe characteristics were recorded by slowly sweeping the probe bias voltage and fixing the aperture of the boxcar integrator to provide temporal resolution. When current was collected continuously, the probe was quickly damaged by sputtering and heating, even in the pulsed discharge. To extend the probe lifetime, a second transistor switch similar to that shown in figure 6(b), but designed for much lower current, was used. This left the probe floating most of the time; typically current was collected for only 50  $\mu$ s during each pulse, and measured for the last 20  $\mu$ s.

To determine space potential, defined as the inflection point in the probe characteristic, derivatives of the probe characteristics were taken. This was done by adding a 2 V peak-to-peak, 50 kHz signal to the probe bias, and performing phase-sensitive detection at that frequency on the probe current (Branner, Friar & Medicus 1963). The response time of the lock-in amplifier was much longer than the resolution desired so, after some filtering and amplification, the signal was gated by a mixer before being applied to the lock-in amplifier. The gate output from the boxcar integrator was sufficient to drive the mixer, ensuring that there was no temporal offset between the probe characteristic and the measurement of its derivative.

Figure 7(a) shows the circuit used for the Langmuir probe diagnostics; figure 7(b) shows typical timing waveforms and identifies the instruments controlling their sequencing.

(iii) RF Measurements

RF emission from the discharge was picked up by a wire loop (see §3.1) and was studied in three modes. Most simply, the signal could be viewed on the oscilloscope on a single shot basis, providing a general indication of the temporal evolution of the emission. Alternatively, a spectrum analyzer (1 kHz - 40 GHz) could be used to perform two types of time-resolved spectroscopy. In the first, the frequency band of the analyzer was fixed, so that it acted as a narrowband power meter. The analyzer output could then be viewed on the oscilloscope, or averaged over many pulses with the boxcar integrator. In the second approach, the frequency band was swept slowly while the aperture of the boxcar integrator

was held at a fixed time relative to the initiation of the current pulse. The spectrum of the RF emission at that time was then recovered.

#### (iv) Microwave Interferometry

The microwave interferometer shown schematically in figure 8 was used to measure electron density. The klystron output (22.5 GHz) would be below cut off for transmission through the discharge for electron densities above  $6.25 \times 10^{12}/\text{cm}^3$ . The attenuator and phase-shifter in the reference arm were adjusted, with the discharge off, to cancel the attenuation of the glass and the differences in path length between the two arms, giving zero voltage difference between the two crystals in the magic-tee detector. When the discharge was on, it introduced additional phase shift and attenuation in the discharge arm of the interferometer. The phase shift could be measured directly by nulling it with the phase-shifter in the reference arm, thus eliminating the effects of attenuation in the discharge.

If the interferometer frequency,  $f_I$ , is much higher than the electron plasma frequency, the electron number density,  $n_p$ , is linear in the phase shift,  $\Delta\phi$ ,

$$n_p = 4 \times 10^{-9} \left( \frac{Gcf_I}{d} \right) \Delta\phi$$

where  $c$  is the speed of light, and  $d$  is the diameter of the discharge column (Heald & Wharton 1965). The numerical factor,  $G$ , of order unity, takes into account two effects. First, the width of the microwave beam perpendicular to the discharge is as large as the column, so that much of the beam traverses only a short chord of the discharge. Second, even if the perpendicular width of the discharge were infinite, the density deduced would be a line-average across the discharge. The factor introduced by radial inhomogeneity depends on the profile, but for parabolic or Bessel function profiles pertinent to Tonks-Langmuir free-fall theory (Tonks & Langmuir 1929) and Schottky isothermal ambipolar diffusion theory (Schottky 1924), respectively, is between 1.2 and 1.6. An empirical value of  $G = 5.0$  was found by calibration against measurements of on-axis densities made with a Langmuir probe.

The response time for the interferometer was limited by the RC time-constant of the diode outputs. When viewed on the oscilloscope, it was

at most 1  $\mu$ s. For the small shifts, and negligible attenuation observed, the voltage difference produced in the magic-tee detector was a linear measure of the electron number density.

#### 4.3. Observations and Measurements

When the discharge current was pulsed from a low level to a high level (typically for 0.1-5.0 ms at 60 Hz-1 kHz), it was observed that more current was drawn for a given anode-to-cathode potential drop than in the steady-state. The discharge took from 20  $\mu$ s to 10 ms to approach steady-state conditions closely, taking longer with higher neutral pressures and larger current pulses.

The presence of a double-layer was indicated by oscillograms such as those of figure 9. The discharge current was pulsed to a high level, which it maintained for a few hundred  $\mu$ s, and then was limited to a lower level, which it maintained for the remainder of the high current pulse. Simultaneous with the onset of current limitation, a short region of the discharge (a few centimeters) could be located that evidenced a large increase in RF emission. The spatial location of this region and the amplitude of the discharge current after current limitation were the same as in the non-pulsed column, suggesting strongly that the double-layers formed were essentially the same in both modes of operation.

Time-resolved studies showed that the RF emissions below 10 MHz grew and saturated simultaneously with the decrease and limitation of the discharge current (see figure 10). The double-layer was associated with noise generation at frequencies near and below the ion plasma frequency,  $\omega_{pi}/2\pi \approx 15$  MHz ( $n \approx 2.0 \times 10^{11}/\text{cm}^3$ ), as shown in figure 11. Fluctuations at higher frequencies, near the electron plasma frequency, were not observed, but since these would not couple efficiently to the capacitive probes, their occurrence is not precluded.

Langmuir probes gave spatially- and temporally-resolved data on the space potential, temperature and electron density within the column. Space potential, defined as the inflection point in the probe characteristic, was determined as the maximum of the derivative curve. The temperature was determined by fitting a straight line to a plot of  $\ln I$  vs  $V$  in the electron retardation region, where  $I$  is the probe current and  $V$  the probe bias voltage. The density was then found from the temperature



and the electron saturation current. The voltage difference between floating and space potential was used as a check on the temperature measurement.

As in the non-pulsed column, the double-layer was strongly perturbed by the presence of the probe in its vicinity. Probe measurements were consequently taken several centimeters away from the double-layer. It was also found that, at the low neutral pressures studied ( $\leq 1$  mTorr), the probe data indicated significant depletion in the high energy tail, and as determined by the  $\ln I$  vs  $V$  method, a very high electron temperature: in excess of 15 eV, instead of the 7-8 eV predicted for an argon positive column at this pressure-radius product (Ilić 1973). Temperatures lower by about a factor of two were found from the difference in floating and space potential, reflecting the depletion of the high energy tail of the electron distribution relative to a Maxwellian. For density determination, temperatures found from the former method were used. This choice is not critical; the density deduced from probe data depends on the reciprocal of the square root of the temperature so that it will decrease by only 30% when the temperature is doubled.

Figure 12 shows the temporal evolution of the space potential, electron temperature and density on each side of a double-layer. Between 300 and 500  $\mu$ s into the pulse, space potential on the anode and cathode sides increased by about 10 V and 2 V, respectively. There was a simultaneous decrease in the discharge current of 1.5 A, which with a load resistance of 8  $\Omega$  corresponded to a voltage increase of 12 V across the entire column. We can consequently deduce from the probe measurements that there was an 8 V increase over a 28 cm length of the narrow column and only a 4 V increase over the rest of the discharge length, i.e. 210 cm, including the remaining 58 cm of the narrow section. The extent of the double-layer region could be further localized to 10 cm by the RF emission.

Microwave interferometer measurements indicated that density and current variations were well correlated, as shown in figure 13. Measurements on both sides of the double-layer showed no significant difference between the two sides. To improve the sensitivity to density differences, the interferometer was reconfigured so that both paths traversed the plasma, one on each side of the double-layer. Even the residual noise level caused by vibration was larger than the signal related to a density difference.

The double-layers just described can be considered to be stable, in the sense that once they form they remain in existence and are localized for the duration of the pulse. They are also weak (Block 1978) since the potential difference across the double-layer is less than, or about equal to, the thermal energy of the plasma. The occurrence of another class of unstable, strong double-layers can be inferred from some current pulses. They appeared as drops in current of as much as 10-12 A, i.e. 80-100 V increases across the column, lasting 50-100  $\mu$ s, as shown in figure 14. These were even more difficult to study than stable double-layers for two reasons. First, the current drops did not develop at the same time in each successive pulse, so that sampling diagnostic techniques could not be used, and second, they regularly extinguished the discharge after a number of current pulses.

## 5. DISCUSSION

The Langmuir probe measurements reported here clearly demonstrate the occurrence of double-layers in an argon positive column. Supplementary evidence consistent with the probe data in pointing to the formation of double-layers was also observed, e.g., the transition in the luminosity; the heating of the walls, the RF generation; the tendency of the double-layer to move toward regions of lower pressure, and its tendency to form at the Langmuir probes when they are within a few centimeters of the region where the double-layer would otherwise form, as reported in positive column experiments with other gases (Armstrong & Torvén 1974; Armstrong 1975; Sandahl, Babić & Torvén 1971; Babić & Torvén 1974; Torvén & Babić 1971).

There are, however, significant points of difference between this and previous experiments. In particular, the double-layers investigated here were weak and stable, rather than strong and unstable, as discussed at the end of § 4. With the low-inductance circuit used, the strong double-layers extinguished the discharge, whereas in other experiments (Torvén & Babić 1971; Babić & Torvén 1974) it has proved possible to maintain the discharge by inserting a large inductor in the external circuit. A plausible interpretation of this is that the double-layer forms in a narrow bounding region of current/pressure parameter space separating relatively low- and high-voltage operation of the discharge. Whether or not a smooth transition can be effected from weak to strong double-layers, by current or pressure variations, then depends critically on the impedances and power supply external to the tube.

It is evidently very difficult to make precise measurements on intermittent, highly unstable, strong double-layers, and it is noteworthy that the experiments described here on weak double-layers clearly associate limitation of the discharge current with double-layer formation, (see § 4.3) an effect not previously reported, and indicate a drift-to-thermal velocity ratio for onset less than 0.3. This ratio can be inferred to be nearer unity in previous experiments on strong double-layers (Babić & Torvén 1974).

A desired outcome of double-layer experimentation is a physical model that can be subjected to mathematical analysis. So far, a sharply defined model has not emerged from our own or previous positive column experiments. Although we have not yet been successful, we shall indicate here the lines

along which we have been proceeding, with the hope that other ideas and analytical work will be stimulated by the discussion.

Two distinctions seem to us to be extremely important: first, between fully-ionized plasmas and partially-ionized discharges (in which volume ionization processes are significant), and second, between infinitely long discharges and those short enough for double-layers to be influenced by the ends.

Theoretical models predict that double-layers can form in fully-ionized plasmas when suitable charged particle populations are present, i.e. electrons and ions reflected by the double-layer, and electrons and ions transmitted (Levine & Crawford 1980). Multiple plasma devices permit such populations to be produced and controlled under effectively fully-ionized conditions, and indeed demonstrate double-layer formation (see § 2.3). It seems likely that ionospheric double-layers also occur in effectively fully-ionized plasma. The question consequently arises as to whether double-layers produced in partially-ionized plasmas are similar in character. This question is sharpened when it is noted that the occurrence of double-layers in multiple-plasma devices is sensitive to the presence of neutral gas (Coakley & Hershkowitz 1979; Coakley, Johnson & Hershkowitz 1979).

The foregoing question could be resolved by measuring the temporal and spatial variations in the electron and ion velocity distributions on each side of a double-layer, and this provided strong initial motivation for the experiments described in this paper. We simply found it prohibitively difficult to make such probe measurements accurately, though many attempts were made. Improved diagnostics, e.g. Langmuir probes with guard-rings, and ion energy analyzers, are bulky, and would necessitate use of much larger diameter tubes. This, in turn, would necessitate much larger currents, to reach double-layer current densities, compounding the problems of cooling the column and pulsing the discharge current. Even if these problems could be solved, it is unclear if the perturbing effects of the probes could be overcome, allowing measurements to be made close to the double-layer. The alternative technique of laser scattering would require even higher charge densities and currents, and be extremely difficult to refine sufficiently. An experimental breakthrough is clearly required if detailed velocity distributions are to be obtained.

Our second distinction is essentially between long and short discharges, and leads to such questions as: (i) Would a series of free double-layers form

in an infinitely long positive column, analogous to the well-known repeated double-layer phenomenon of striations, typically observed at much higher pressures? (ii) Could a single double-layer form in an infinitely long positive column, effectively separating two columns with different parameters? (iii) Does a double-layer mark a transition region between sections of a discharge materially influenced by the ends?

Since spatially periodic series of double-layers have not been observed, either in our own or previous work, and because mean free paths for collisional ionization are not generally negligible compared with the distances between double-layers and electrodes, our thinking has concentrated on the third question. We have assumed in our model that the discharge current is first carried by primary electrons from the cathode, and that these are progressively slowed down in ionizing collisions, and lost to the discharge wall. We have carried out computations to establish whether a region is reached in which a rapid increase in energy, via a double-layer analogous to a striation double-layer, is required to produce more ionization. We speculate that at lower currents and higher pressures the cathode region is joined smoothly to a self-sustaining positive column, without the formation of a double-layer.

Our calculations along the foregoing lines have concentrated on the ionization balance and electric field distribution as current and pressure are varied, but so far the double-layer phenomenon has not been observed in the numerical results. Whether or not this is a defect of the model, or failure to locate parameters corresponding to the narrow range in which double-layers are observed experimentally, is not yet clear.

Alternative explanations which require new and extensive experimentation involve neutral depletion (starvation) of the column. The double-layer may constitute a localized form of discharge extinction (Stangeby & Allen 1971), where a minimum in the neutral density occurs, either due to the manner in which the neutral gas is introduced into the discharge, or to the neutral pumping by the discharge current (Rosa & Allen 1970). We have tended to ignore such mechanisms since our positive columns are typically only a few per cent ionized. To resolve the question, spatial and temporal measurements of neutral density would be required in addition to the charged particle velocity distribution measurements proposed above for future work.

Acknowledgments: Comments and advice from Dr. D. B. Ilić on the various phases of this research were greatly appreciated. The work was supported by the National Aeronautics and Space Administration, and the National Science Foundation.

## REFERENCES

- ANDERSSON, D. 1978 Report No. 78-103 Royal Institute of Technology, Department of Electron Physics, Stockholm.
- ANDERSSON, D., BABIĆ, M., SANDAHL, S. & TORVÉN, S. 1969 Proceedings of 9th International Conference on Phenomena in Ionized Gases, p. 142. Academy of the Socialist Republic of Romania.
- ARMSTRONG, R. J. 1975 Proceedings of 12th International Conference on Phenomena in Ionized Gases, p. 124. North Holland.
- ARMSTRONG, R. J. & TORVÉN, S. 1974 Report No. 10-74. The Auroral Observatory, Tromsø.
- BABIĆ, M., SANDAHL, S. & TORVÉN, S. 1971 Proceedings of 10th International Conference on Phenomena in Ionized Gases, p. 120. Donald Parsons.
- BABIĆ, M. & TORVÉN, S. 1974 Report TRITA-EPP-74-02. Royal Institute of Technology, Department of Electron Physics, Stockholm.
- BLOCK, L. P. 1978 Astrophys. Space Sci. **55**, 59.
- BOHM, D. 1949 The Characteristics of Electrical Discharges in Magnetic Fields (ed. A. Guthrie & R. K. Wakerling), p. 77. McGraw-Hill.
- BRANNER, G. R., FRIAR, E. M. & MEDICUS, G. 1963 Rev. Sci. Instr. **28**, 822.
- CARIQVIST, P. 1979 Wave Instabilities in Space Plasmas (ed. P. J. Palmadesso & K. Papadopoulos). Reidel, p. 83.
- COAKLEY, P. & HERSHKOWITZ, N. 1979 Phys. Fluids, **22**, 1171.
- COAKLEY, P. HERSHKOWITZ, N., HUBBARD, R. & JOYCE, G. 1978 Phys. Rev. Lett., **40**, 230.
- COAKLEY, P., JOHNSON, L. & HERSHKOWITZ, N. 1979 Phys. Lett., **70A**, 425.
- CRAWFORD, F. W. & CANNARA, A. B. 1965 J. Appl. Phys., **36**, 3135.
- CRAWFORD, F. W. & FREESTON, I. L. 1963 Proceedings of 6th International Conference on Phenomena in Ionized Gases, p. 461. SERMA.
- HEALD, M. A. & WHARTON, C. B. 1965 Plasma Diagnostics with Microwaves, p. 120. J. Wiley & Sons.
- ILIĆ, D. 1973 J. Appl. Phys., **44**, 3993.
- JACOBSEN, R. A. & EUBANK, H. P. 1973 Plasma Phys., **15**, 243.
- LANGMUIR, I. 1929 Phys. Rev., **33**, 954.
- LEVINE, J. S. & CRAWFORD, F. W. 1980 J. Plasma Phys. (in press).
- LUTSENKO, E. I., SEREDA, N. D. & KONTSEVOI, L. M. 1976 Soviet Phys. Tech. Phys., **20**, 498.

- OLESON, N. L. & COOPER, A. W. 1968 Advances in Electronics and Electron Phys., 24, 155.
- PREWETT, P. D. & ALLEN, J. E. 1976 Proc. Roy. Soc., A348, 435.
- QUON, B. H. & WONG, A. Y. 1976 Phys. Rev. Lett., 37, 1393.
- RAYMENT, S. W. & TWIDDY, N. D. 1969 J. Phys., D2, 1747.
- ROSA, R. & ALLEN, J. E. 1970 J. Phys., D3, 184.
- SANDAHL, S. 1971 Physica Scripta, 3, 275.
- SCHOTTKY, W. 1924 Phys. Z., 25, 635.
- SELF, S. A. 1965 J. Appl. Phys., 36, 456.
- STANGEBY, P. C. & ALLEN, J. E. 1971 J. Phys., A4, 108.
- TONKS, L. & LANGMUIR, I. 1929 Phys. Rev., 34, 876.
- TORVÉN, S. 1979 Wave Instabilities in Space Plasmas (ed. P. J. Palmadesso & K. Papadopoulos). Reidel, p. 109.
- TORVÉN, S. & ANDERSSON, D. 1979 J. Phys., D12, 717.
- TORVÉN, S. & BABIĆ, M. 1971 Report No. 71-20, Royal Institute of Technology, Division of Electron Physics, Stockholm.
- TORVÉN, S. & BABIĆ, M. 1973 J. Phys., E6, 442.



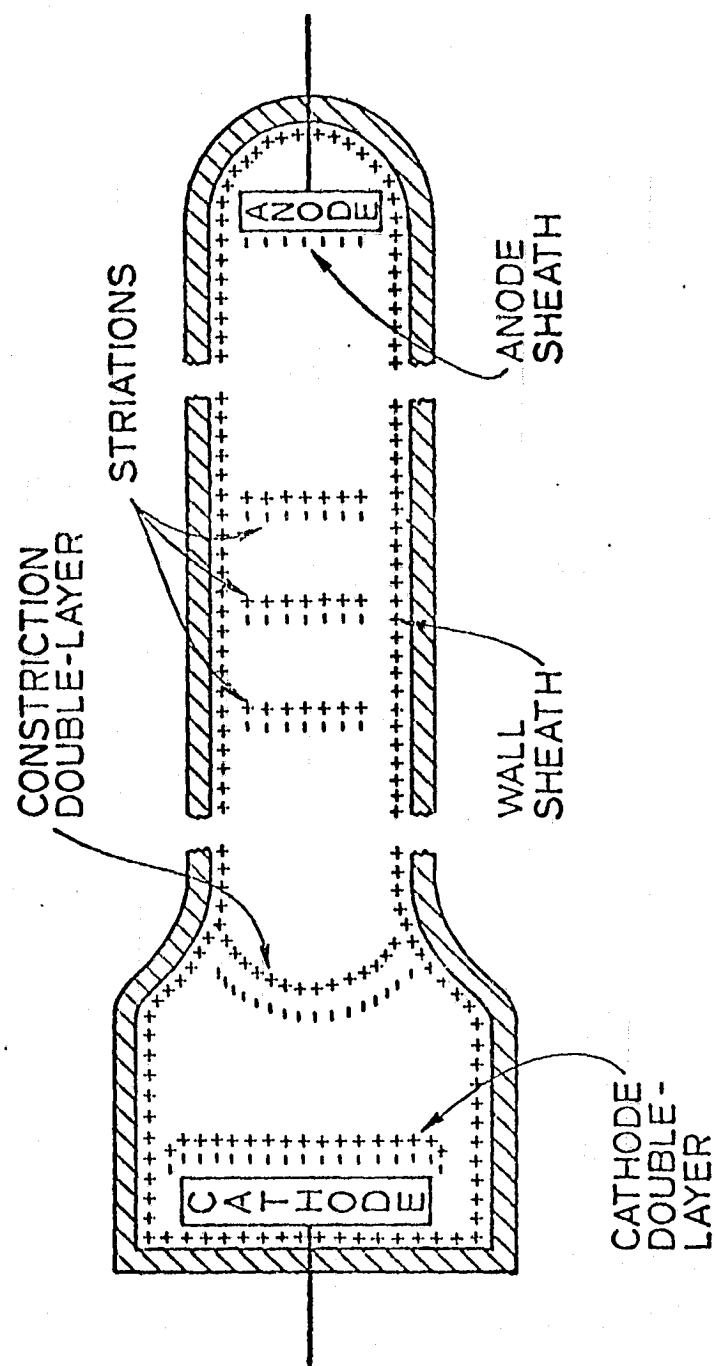
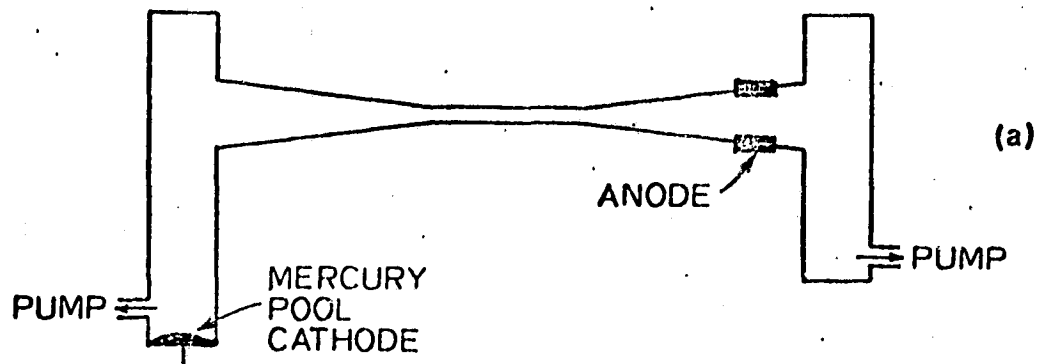
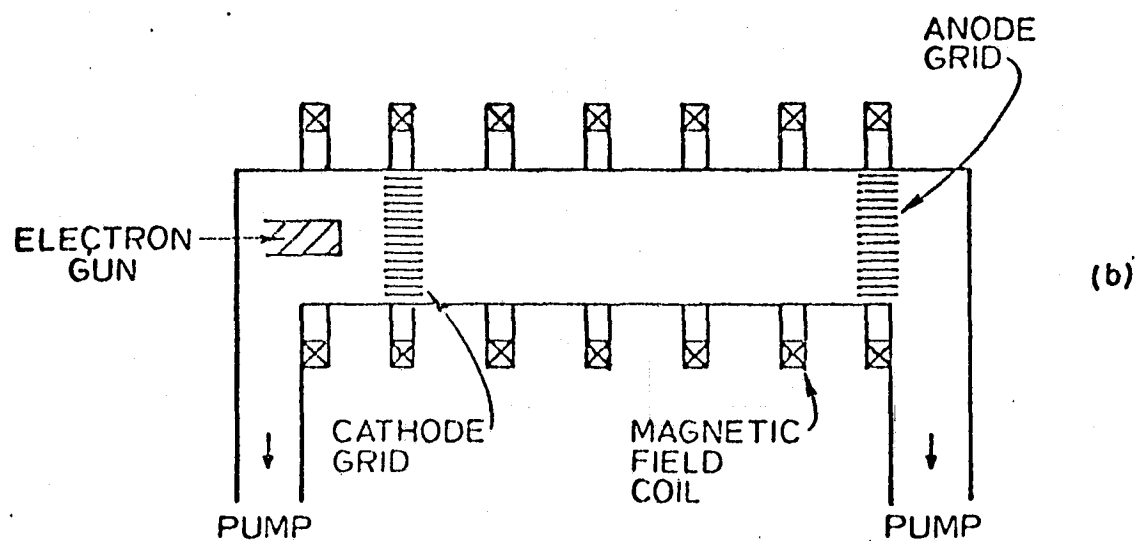


FIG. 1. Sheaths and double-layers commonly observed in low-pressure discharges.

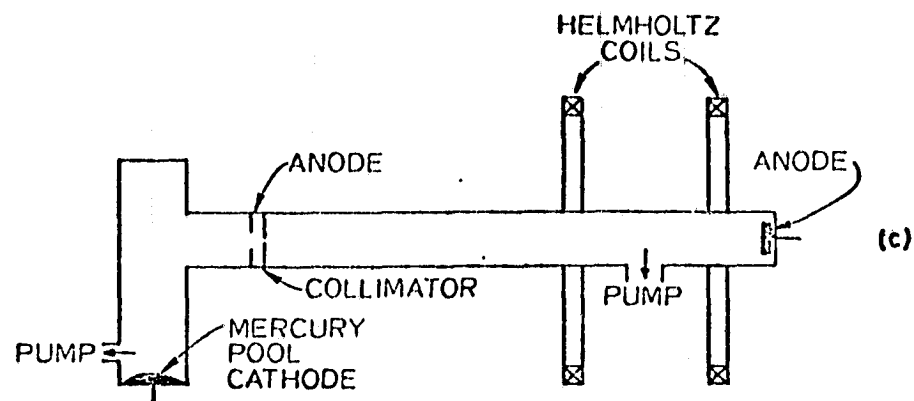


(a) Mercury-vapor positive column discharge with tapered sections.

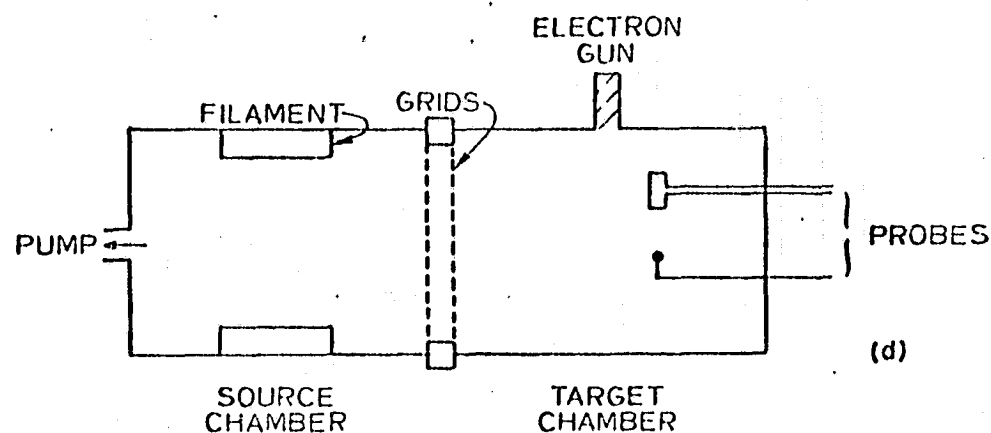


(b) Linear discharge in a magnetic field.

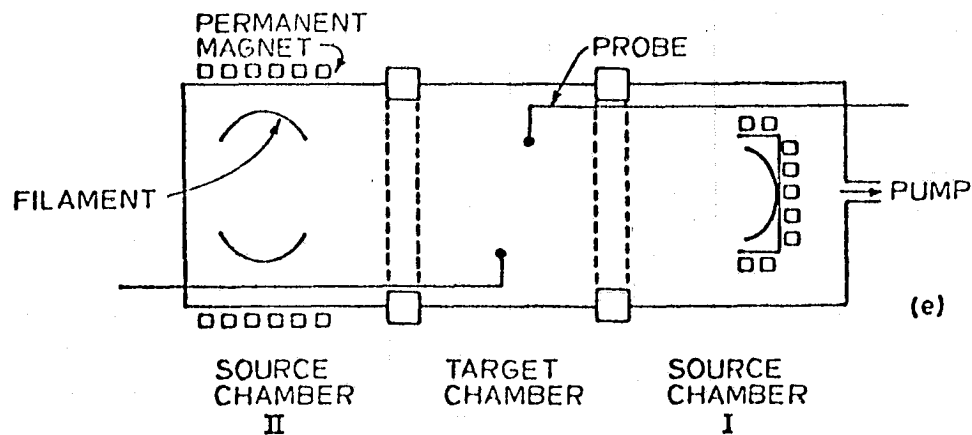
FIG. 2. Apparatus used in previous double-layer investigations.



(c) Diffusion column in a magnetic field.



(d) Double-plasma device.



(e) Triple-plasma device.

FIG. 2. (Contd.) Apparatus used in previous double-layer investigations.

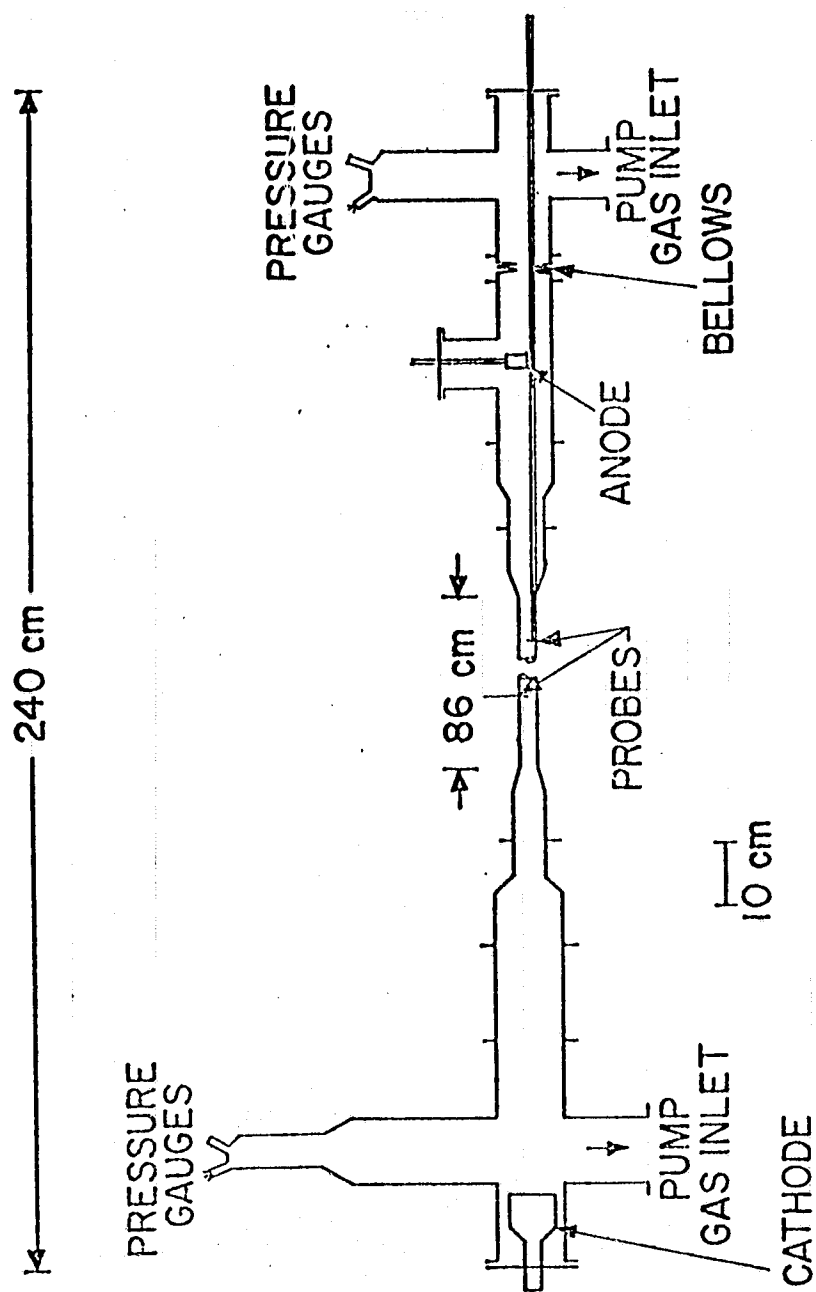


FIG. 3. Apparatus for double-layer investigation.

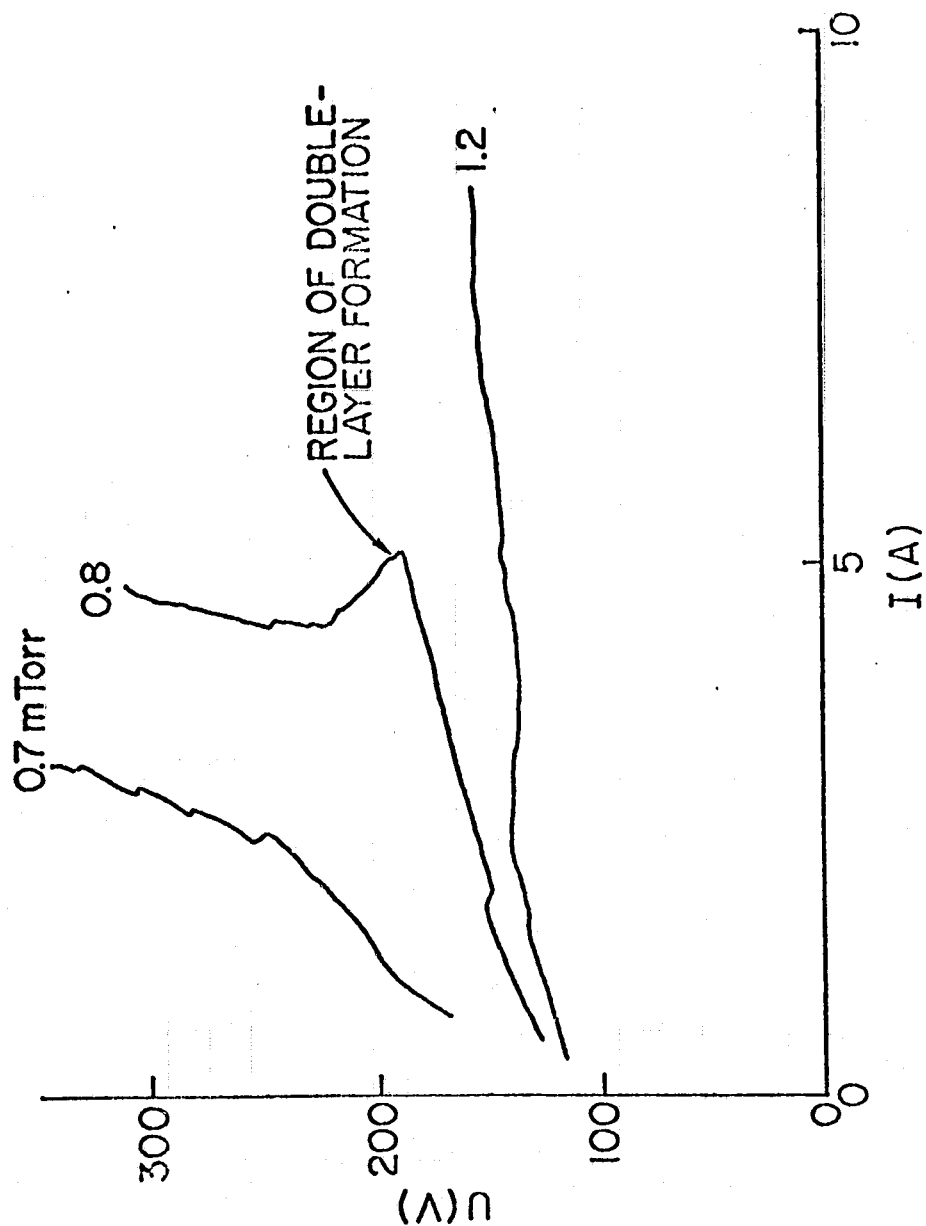


FIG. 4. Current-voltage characteristics of an argon positive column.  
(Double-layer formation is associated with the abrupt transition in the 0.8 mTorr curve.)

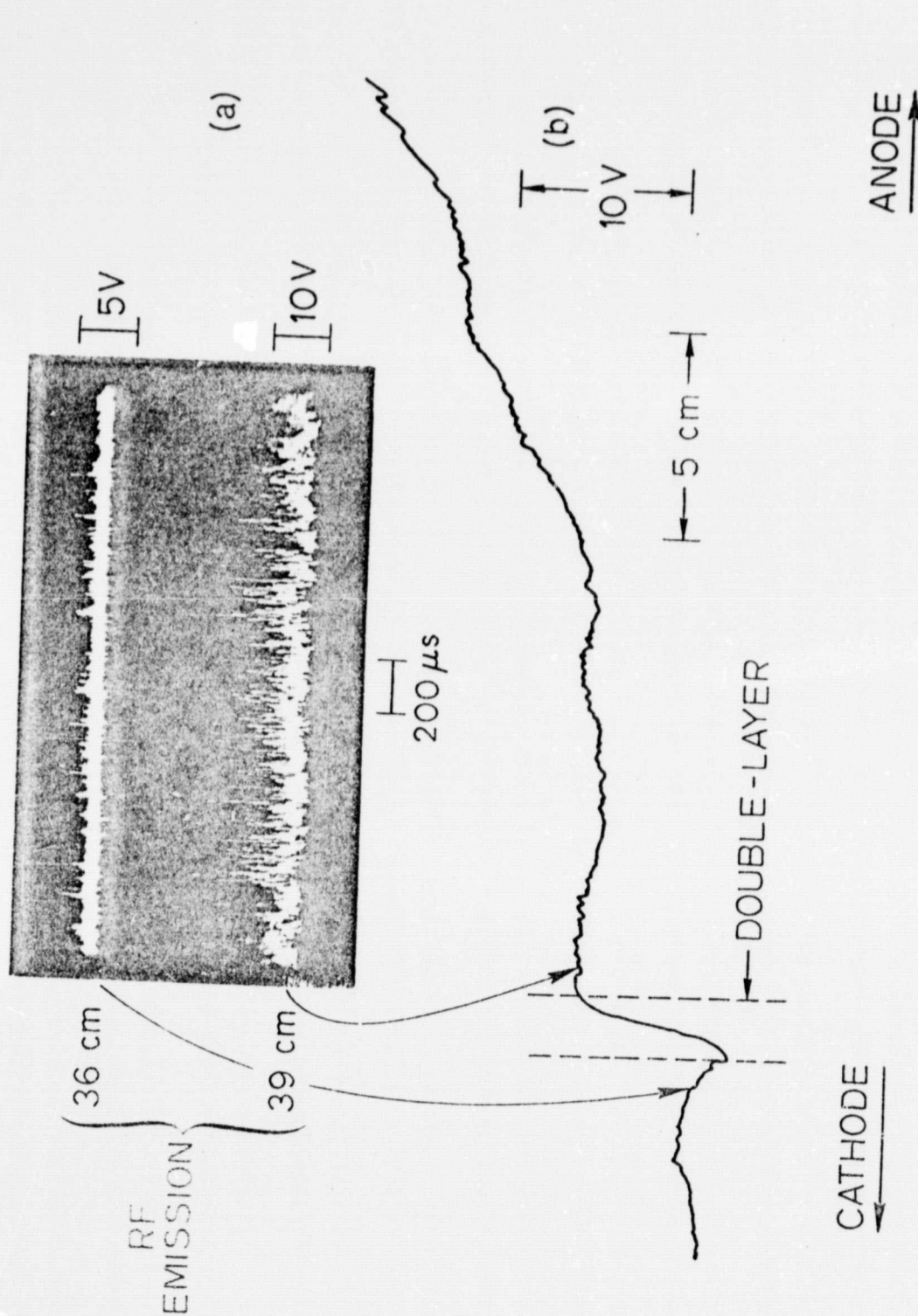


FIG. 5. Steady-state double-layer.

(a) RF emission on cathode and anode sides of a double-layer ( $P_{\text{CATH}} = 2.6$  mTorr;  $P_{\text{ANODE}} = 0.74$  mTorr;  $U = 168$  V;  $I = 7.9$  A),

(b) Axial variation of the floating potential of a Langmuir probe in the vicinity of a double-layer ( $P_{\text{CATH}} = 2.2$  mTorr;  $P_{\text{ANODE}} = 0.51$  mTorr;  $U = 145$  V;  $I = 5.0$  A).

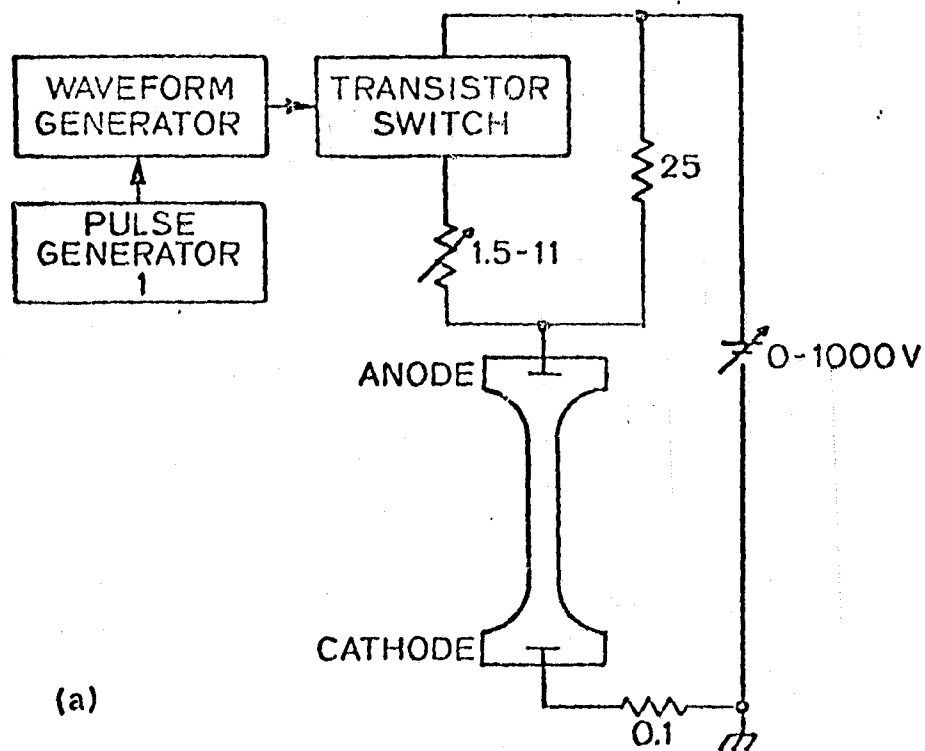


FIG. 6(a). Circuit for the pulsed discharge.  
(Resistances are in  $\Omega$ .)

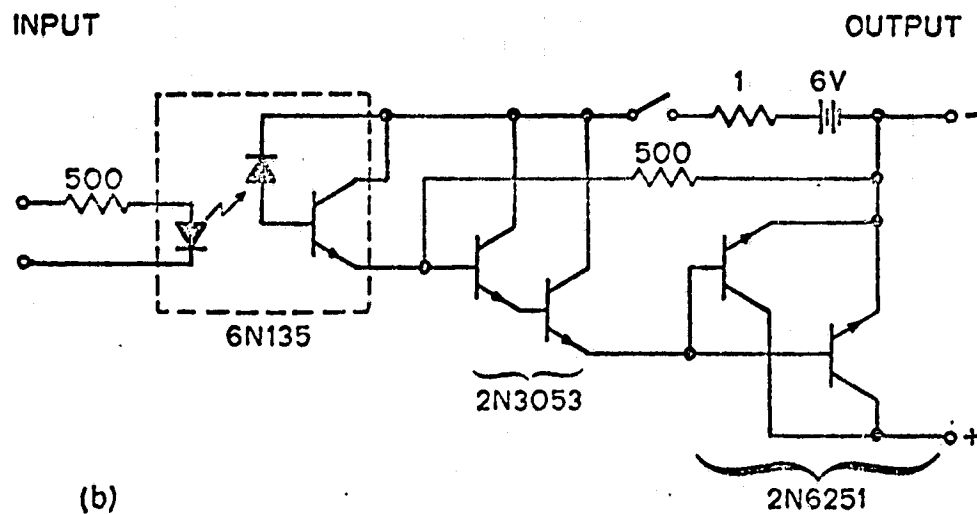


FIG. 6(b). Detail of the transistor switch.  
(Resistances are in  $\Omega$ .)



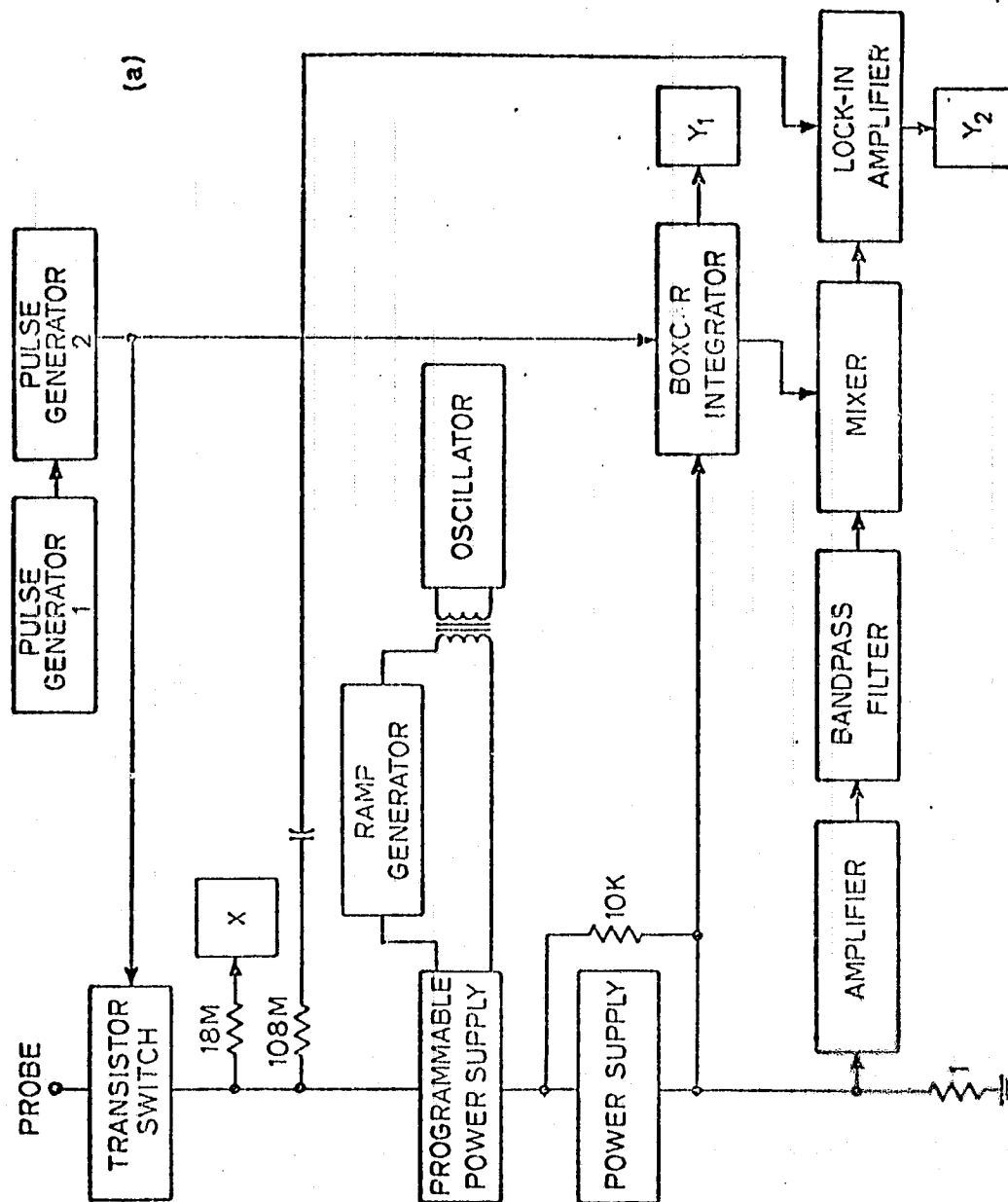


FIG. 7(a). Circuit for probe diagnostics in the pulsed discharge.  
 ( $X$ ,  $Y_1$  and  $Y_2$  are the axes of XY recorders. Resistances  
 are in  $\Omega$ ).

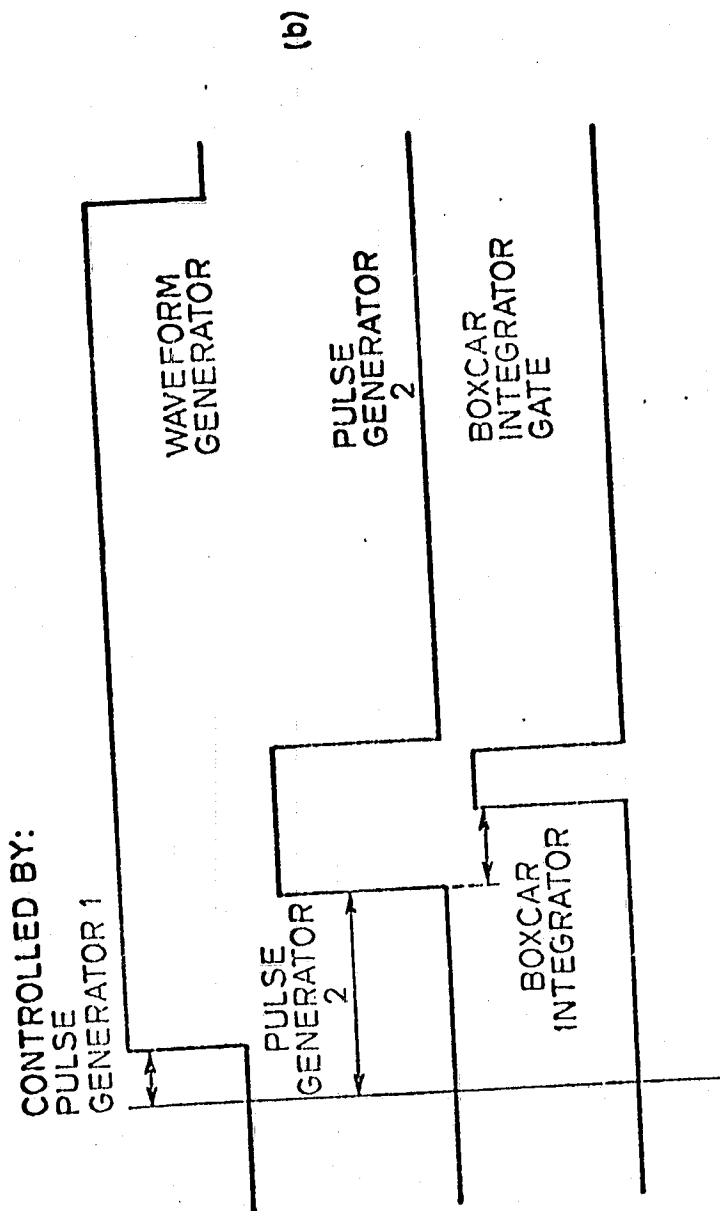


FIG. 7(b). Sequencing diagram of timing pulses. (Reference point is trigger output of Pulse Generator 1.)



ORIGINAL PAGE IS  
OF POOR QUALITY

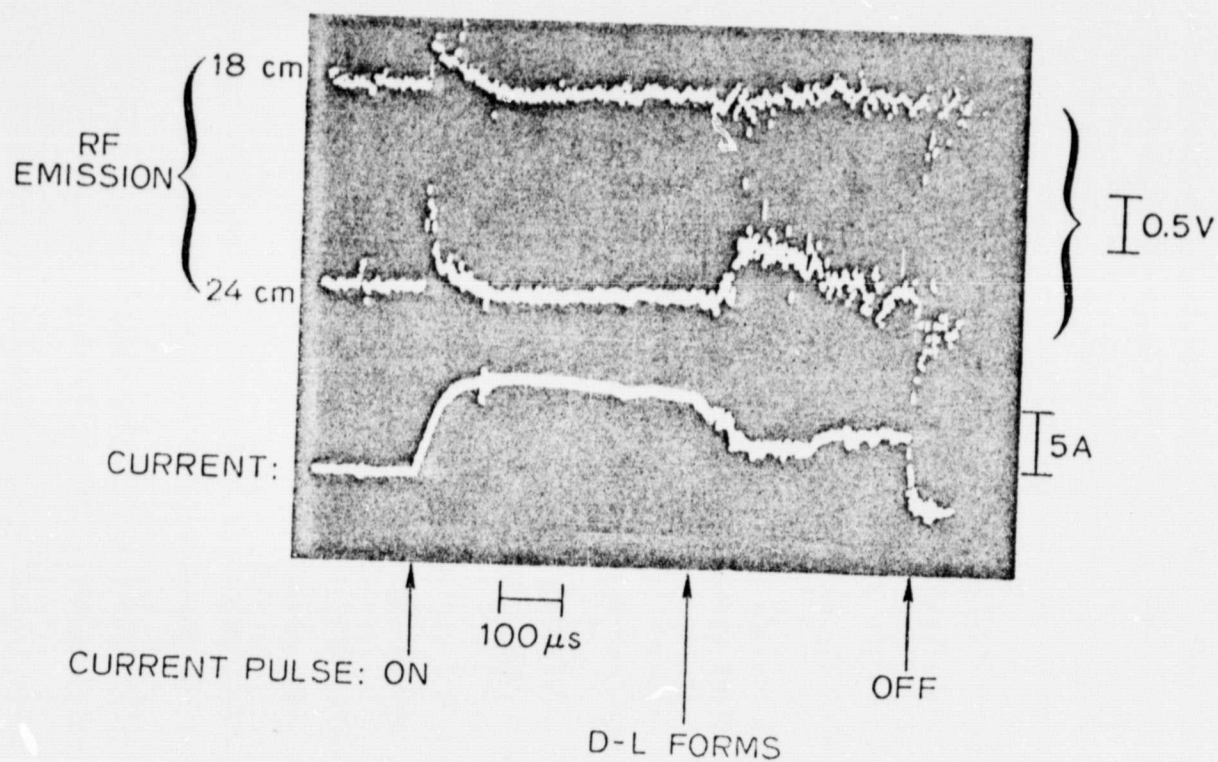


FIG. 9. Pulsed double-layer: RF emission on cathode and anode side of the double-layer, and the discharge current ( $P_{\text{CATH}} = 1.1$  mTorr;  $P_{\text{ANODE}} = 0.57$  mTorr).

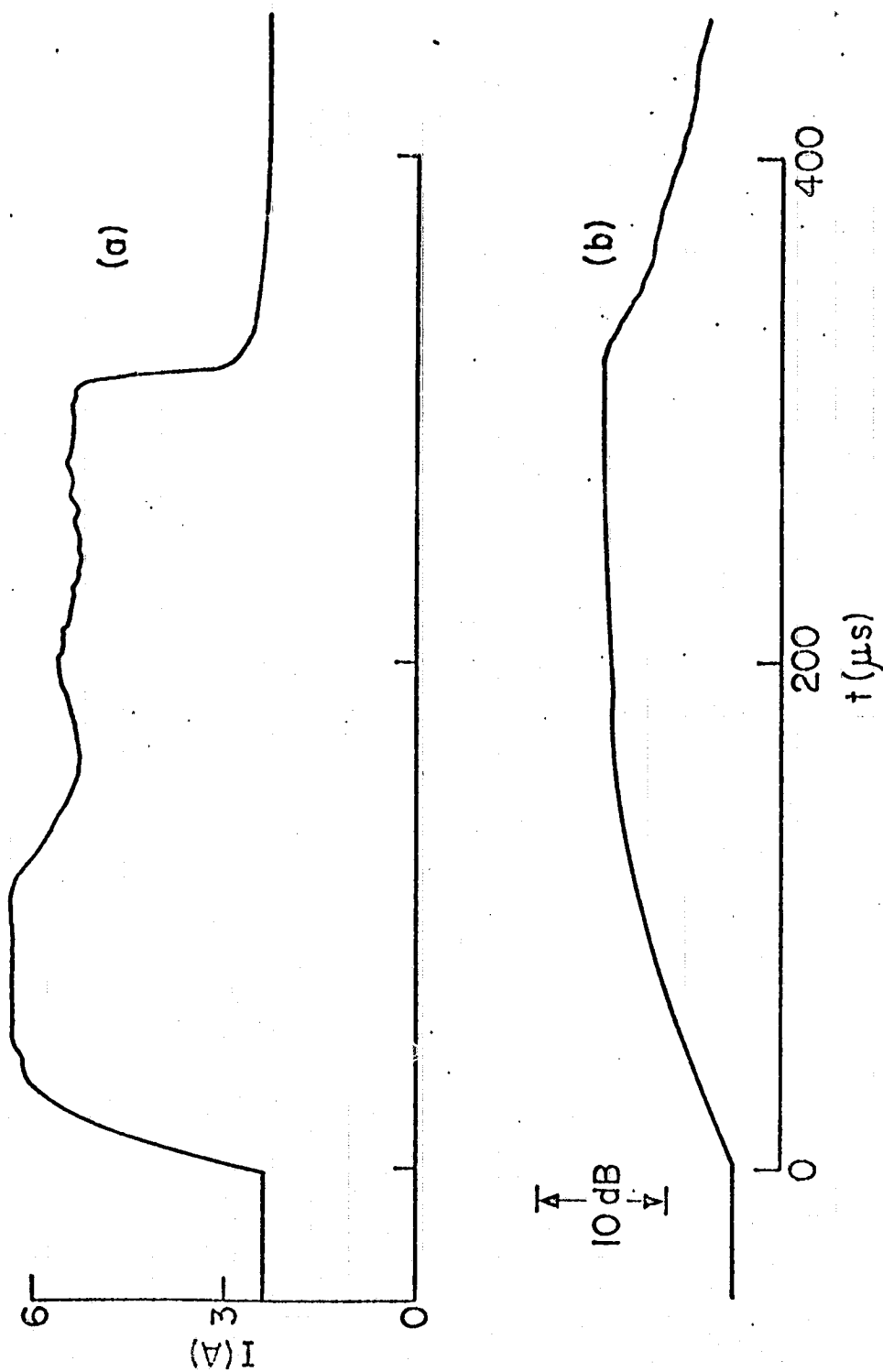


FIG. 10. RF growth and saturation with double-layer formation  
(1.8 MHz ; 300 kHz IF bandwidth;

$P_{\text{CATH}} = 1.8$  mTorr ;  $P_{\text{ANODE}} = 0.18$  mTorr).

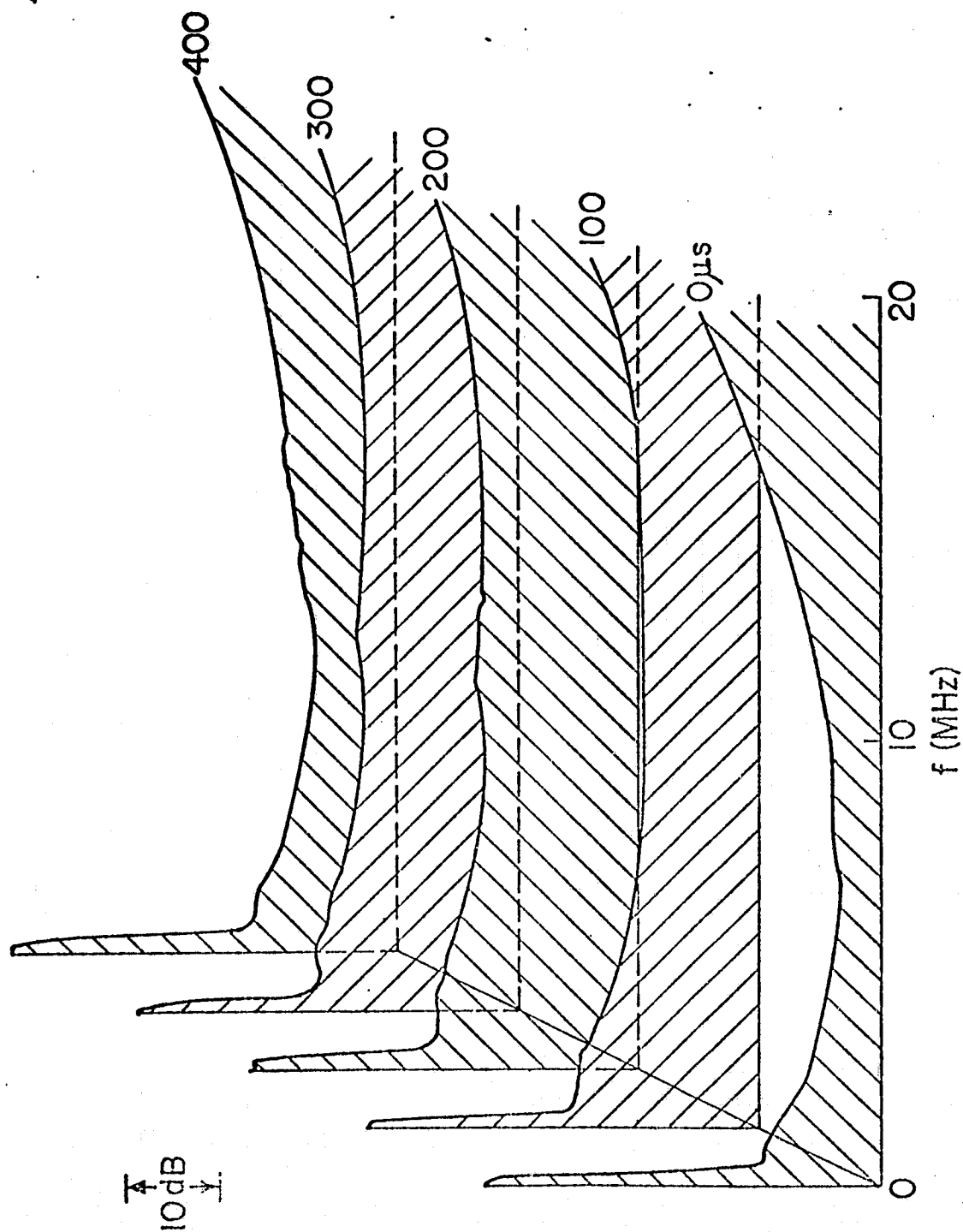


FIG. 11. Low frequency RF generation near double-layer  
 ( $P_{\text{CATH}} = 1.8 \text{ mTorr}$  ;  $P_{\text{ANODE}} = 0.18 \text{ mTorr}$ ).

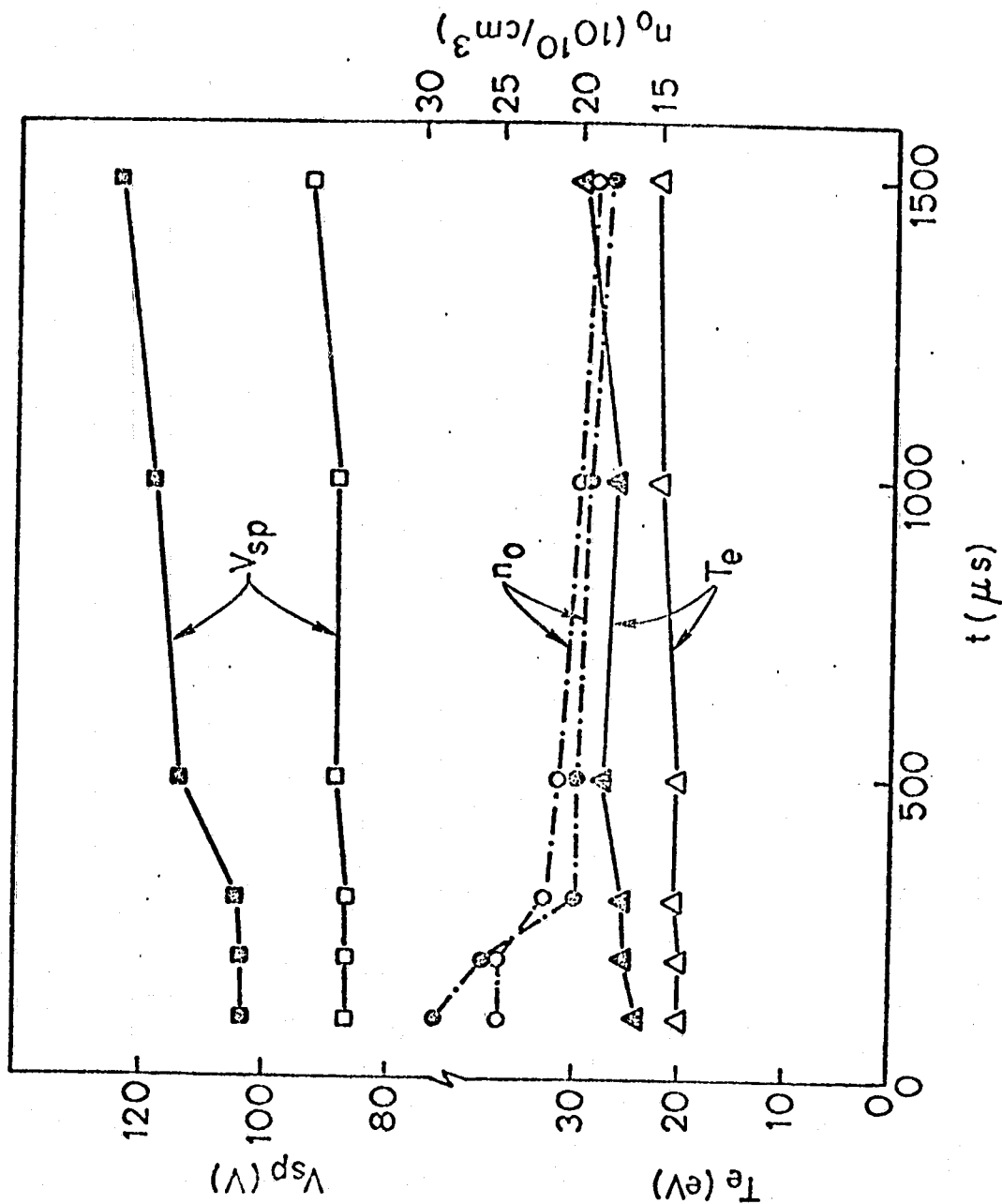


FIG. 12. Time-resolved measurements of space potential, electron temperature and density on the cathode (open symbols) and anode (closed symbols) sides of a double-layer ( $P_{CATH} = 0.96$  mTorr ;  $P_{ANODE} = 0.44$  mTorr).

ORIGINAL PAGE IS  
OF POOR QUALITY

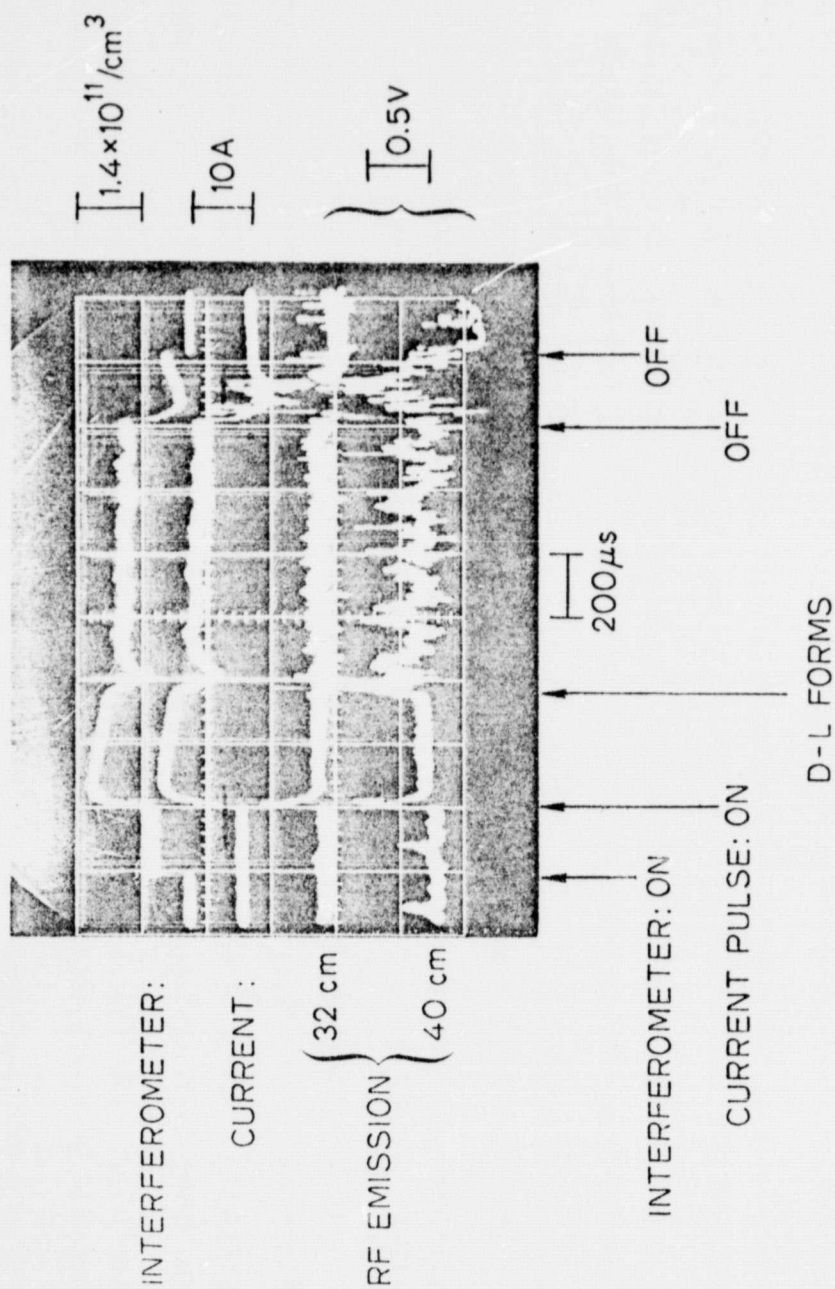


FIG. 13. Pulsed double-layer: Electron density, discharge current and RF emission on cathode and anode sides ( $P_{\text{CATH}} = 0.96 \text{ mTorr}$ ;  $P_{\text{ANODE}} = 0.44 \text{ mTorr}$ ).



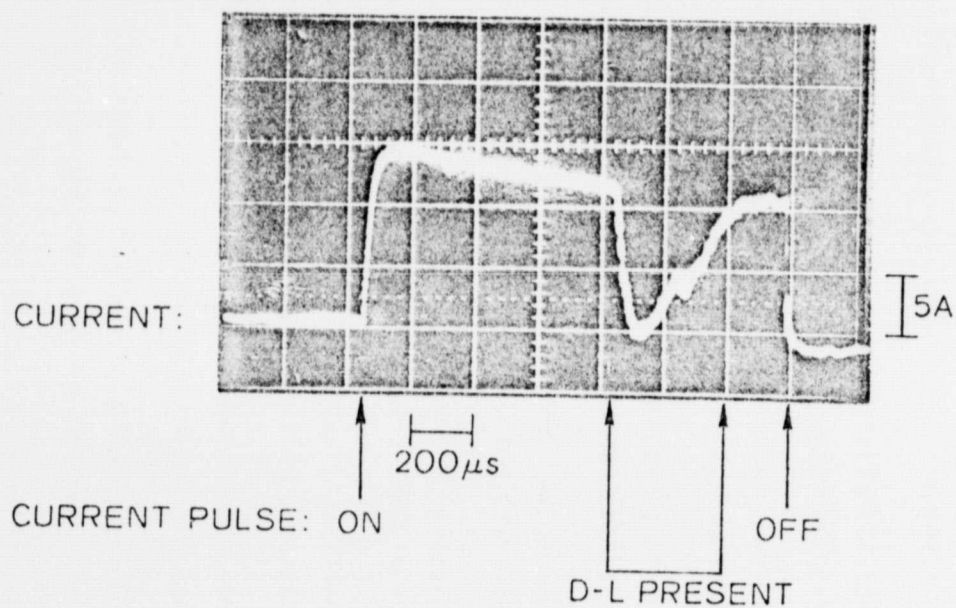


FIG. 14. Discharge current for a strong, unstable double-layer  
 ( $P_{\text{CATH}} = 1.1$  mTorr  $P_{\text{ANODE}} = 0.32$  mTorr).